

Anomalous charge transport phenomena in molecular-based magnet $V(\text{TCNE})_x \cdot y(\text{solvent})$

G. Du, J. Joo, and A. J. Epstein

Department of Physics, The Ohio State University, Columbus, OH 43210-1106

Joel S. Miller

Science and Engineering Laboratories, The Du Pont Company, Wilmington, DE 19880-0328

We present charge transport studies on recently developed molecular-based magnets $V(\text{TCNE})_x \cdot y(\text{solvent})$ (TCNE=tetracyanoethylene) which show local magnetic ordering at temperatures, T , as high as 400 K. $V(\text{TCNE})_x \cdot y(\text{solvent})$ prepared from the solvent CH_2Cl_2 has $\sigma(300 \text{ K}) \sim 10^{-3} \text{ S/cm}$, and that prepared from the solvent CH_3CN has $\sigma(300 \text{ K}) \sim 10^{-5} \text{ S/cm}$. The $\sigma(T)$ of both materials follows the Mott 3D variable range hopping [$\log(T^{1/2}\sigma) \propto T^{-1/4}$] behavior. An anomalously strong T -dependent ac conductivity is likely caused by the short-range ferrimagnetic correlations. Cole-Cole analysis of the ac complex dielectric constant suggests there are two relaxation mechanisms, with an Arrhenius relation fitted to both. The microwave frequency response is consistent with audio frequency data and yields a localization length of $\sim 5 \text{ \AA}$, comparable with the dimensions of a $[\text{TCNE}]^-$ group.

INTRODUCTION

Long-range magnetic ordering at high temperature has been extensively pursued in synthetic molecular-based magnets¹⁻⁴ over the past several years. Magnetic studies show that the recently developed $V(\text{TCNE})_x \cdot y(\text{solvent})$ prepared from various solvents (for example, CH_2Cl_2 , CH_3CN , and THF) has ferrimagnetic correlations at temperatures as high as the decomposition temperature (350 K).⁵ Correlated spin glass and ferrimagnet with wandering axis models were employed to explain the magnetic phenomena.⁶ This local magnetic correlation adds a new element to the local electronic interactions in these materials, which may well influence charge transport.

We present the results of charge transport studies of $V(\text{TCNE})_x \cdot y(\text{CH}_2\text{Cl}_2)$ and $V(\text{TCNE})_x \cdot y(\text{CH}_3\text{CN})$. These materials are semiconductors at room temperature. The conductivity is in accord with Mott's 3D variable range hopping model suggesting that the electronic states are strongly localized. Its magnitude is in the range of many amorphous materials.⁷ However, for $V(\text{TCNE})_x \cdot y(\text{solvent})$, the T -dependence of the audio frequency and the microwave frequency conductivities are observed to be stronger than that predicted by the pairwise hopping model.⁸ It is proposed that this anomaly is likely due to the extreme short-range spin correlations and the Pauli exclusion principle requiring additional thermal energy for a spin-flip process to allow the electrons to hop to nearby (probably nearest-neighbor) sites. This anomalous behavior is absent in amorphous semiconductors and polymers, such as polyaniline, PBO (*p*-phenylenebenzobisoxazole), and BBL (benzimidazobenzophenanthroline) studied earlier.⁹ Cole-Cole analysis¹⁰ of the ac complex dielectric constant showed an unusual feature of two relaxation processes. A small localization length ($\sim 5 \text{ \AA}$) is obtained from the microwave frequency dielectric constant, about the size of a $[\text{TCNE}]^-$ unit, consistent with the strong localization model.

EXPERIMENTAL METHODS

$V(\text{TCNE})_x \cdot y(\text{solvent})$ powder was pressed into pellets for dc and audio frequency conductivity measurements. The sample handling was performed under inert atmosphere conditions due to its sensitivity to air. For the dc measurements, a four-probe technique was used. In the audio frequency (10 Hz–100 kHz) range, a two-probe bridge technique was utilized. The microwave frequency (9–13 GHz) measurements employed the complex bridge technique. Detailed descriptions of the techniques have been reported previously.¹¹⁻¹³

EXPERIMENTAL RESULTS AND DISCUSSION

$V(\text{TCNE})_x \cdot y(\text{CH}_2\text{Cl}_2)$ is a semiconductor with $\sigma(300 \text{ K}) \sim 10^{-3} \text{ S/cm}$, while $V(\text{TCNE})_x \cdot y(\text{CH}_3\text{CN})$ has $\sigma(300 \text{ K}) \sim 10^{-5} \text{ S/cm}$. Figure 1 shows the conductivity plotted as $T^{1/2}\sigma(T)$ vs $T^{-1/4}$. There is a good fit for both materials to Mott's 3D variable range hopping model.⁷

$$\sigma \propto T^{-1/2} \exp[-(T_0/T)^{1/4}],$$

$$T_0 \approx \frac{16\alpha^3}{kN(E_F)}, \quad (1)$$

within the measurable temperature range [90–300 K for $V(\text{TCNE})_x \cdot y(\text{CH}_2\text{Cl}_2)$, and 210–310 K for $V(\text{TCNE})_x \cdot y(\text{CH}_3\text{CN})$] with $T_0 \sim 1.9 \times 10^7 \text{ K}$ for $V(\text{TCNE})_x \cdot y(\text{CH}_2\text{Cl}_2)$ and $T_0 \sim 1.3 \times 10^8 \text{ K}$ for $V(\text{TCNE})_x \cdot y(\text{CH}_3\text{CN})$. These values are typical for poorly conducting disordered materials.¹⁴ The lower σ and larger T_0 of $V(\text{TCNE})_x \cdot y(\text{CH}_3\text{CN})$ imply that its electronic states involved in charge transport are more localized and/or more dilute than those of $V(\text{TCNE})_x \cdot y(\text{CH}_2\text{Cl}_2)$.

The corresponding ac conductivity in the strongly localized regime is often described by the "pairwise" hopping model, i.e., electrons hopping between nearby localized sites,⁸

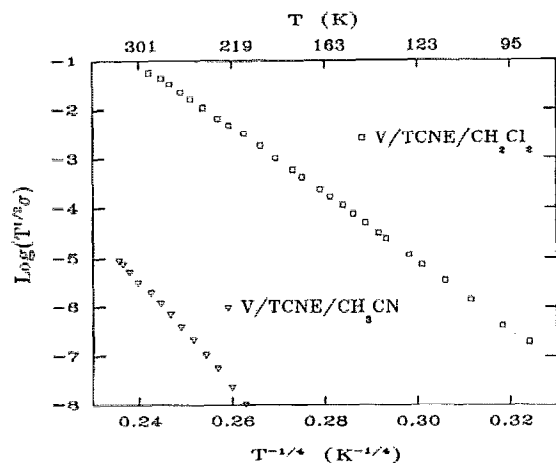


FIG. 1. Temperature dependence of dc conductivity of $V(\text{TCNE})_x \cdot y(\text{CH}_2\text{Cl}_2)$ and $V(\text{TCNE})_x \cdot y(\text{CH}_3\text{CN})$ plotted for comparison to Mott's variable range hopping model.

$$\sigma_{\text{total}}(\omega, T) = \sigma_{\text{dc}}(T) + \sigma_p(\omega, T), \quad (2)$$

where p denotes pair approximation, $\omega = 2\pi f$, and

$$\sigma_p(\omega, T) \propto \omega^s T^n, \quad (3)$$

with $n=1$ and $s \sim 0.8$. Figure 2 shows the ac conductivity versus frequency f (10 Hz–10 GHz) at different temperatures (80–260 K) for $V(\text{TCNE})_x \cdot y(\text{CH}_2\text{Cl}_2)$. The asymptotic behavior at high frequency yields $s \sim 0.7$, in the usual range. However, a plot of $\log[\sigma_p(T)]$ vs $\log(T)$ at 100 kHz (Fig. 3) yields $n \approx 5$, considerably larger than usual. Similar ac results were obtained for $V(\text{TCNE})_x \cdot y(\text{CH}_3\text{CN})$.

The origin of this anomalously large n is of particular interest. We recall from Mott's variable range hopping model⁷ that the hopping rate of an electron between two nearby localized states p_{ij} is

$$p_{ij} \propto \exp(-\alpha R_{ij} - \Delta E_{ij}/k_B T), \quad (4)$$

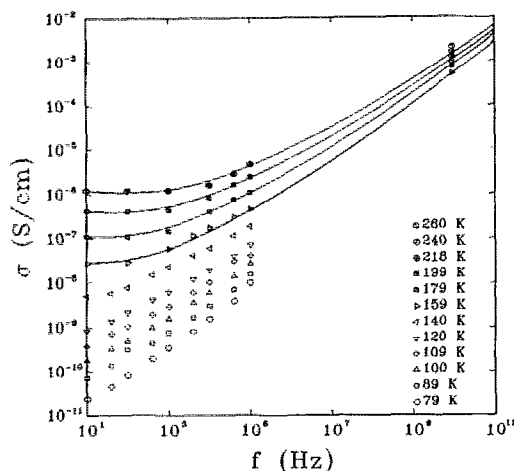


FIG. 2. Frequency dependence of conductivity at different temperatures of $V(\text{TCNE})_x \cdot y(\text{CH}_2\text{Cl}_2)$. Solid lines are guides for the eye. The asymptote of these lines at high-frequency yields $s \approx 0.7$.

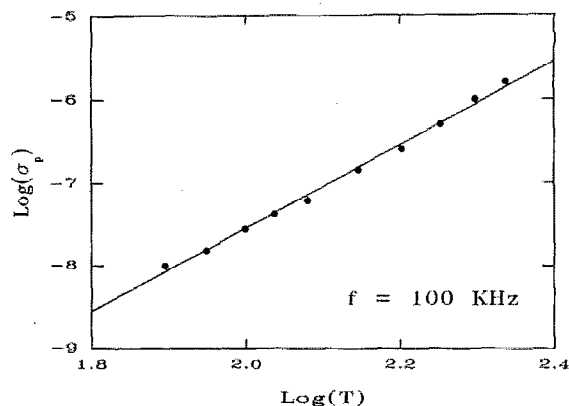


FIG. 3. Temperature dependence of $\sigma_p(T)$ at $f=100$ kHz from Fig. 2. The linear fit yields $n \approx 5$.

where R_{ij} is the hopping distance, ΔE_{ij} is the energy difference between the two states and α^{-1} is the electronic localization length. Mott's model [Eq. (1)] is obtained by maximizing this rate. The local magnetic spin correlation in these magnetic compounds should add an additional term in Eq. (4) for the nearby hops to account for the emission (or absorption) of a spin-flip phonon. Representing the energy involved in the spin-flip process by δ ,

$$p_{ij} \propto \exp(-\alpha R_{ij} - \Delta E_{ij}/k_B T - \delta/k_B T). \quad (5)$$

This additional energy should dominate ΔE_{ij} for the nearby sites (within a radius of ξ , the spin correlation length) introducing a stronger temperature dependence in the ac conductivity. It is interesting to compare the ac case with the dc case, where Mott's 3D variable range hopping model still holds. Here, an electron does not necessarily hop to a nearby site and overcome a larger energy barrier, but rather may hop to a distant site ($R_{ij} > \xi$) with a smaller energy difference and where the magnetic correlation disappears for these systems. The existence of this anomaly at temperatures above T_c in $V(\text{TCNE})_x \cdot y(\text{CH}_3\text{CN})$ [$T_c \approx 150$ K (Ref. 6)] implies that the range of this spin correlation that affects ac charge transport can be small, probably comparable to the size of the nearest-neighbor distance, since n is still large for $V(\text{TCNE})_x \cdot y(\text{CH}_3\text{CN})$ at temperatures higher than 150 K.

The complex dielectric constant may be described by a Cole-Cole relation:¹⁰

$$\epsilon = \epsilon' - i\epsilon'' = \frac{\text{Const}}{1 + (i\omega\tau)^{1-\beta}}, \quad (6)$$

where τ is the relaxation time and β is normally a weak function of temperature for a single Debye-like system.¹⁵ The Cole-Cole analysis of $V(\text{TCNE})_x \cdot y(\text{CH}_2\text{Cl}_2)$ at 120 K, Fig. 4, shows two semicircular arc features (compare with earlier studies on pristine polyaniline and PBO polymers, with only one semicircle⁹), corresponding to two types of nearby-site hops, or two relaxation mechanisms. We speculate that one mechanism is faster in time and shorter in distance, while the other is slower in time and

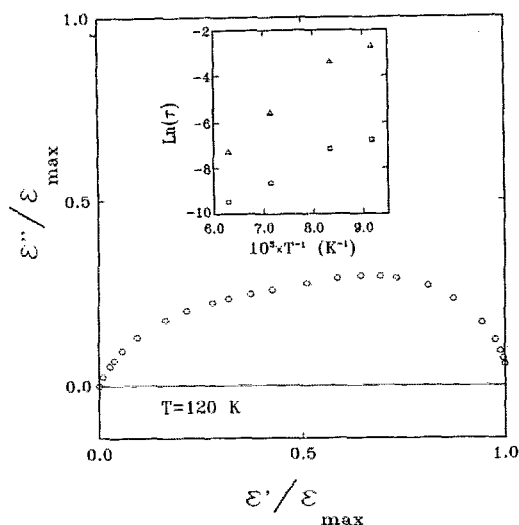


FIG. 4. Cole-Cole plot of $V(\text{TCNE})_x \cdot y(\text{CH}_2\text{Cl}_2)$ at $T=120$ K [$\epsilon_{\text{max}} = \text{Max}(\epsilon', \epsilon'')$]. Inset plots fitting of the Arrhenius relation to the two relaxation processes, \square for the fast one and \triangle for the slow one.

longer in distance. The inset of Fig. 4 represents τ as a function of temperature, via the Arrhenius relation,

$$\tau(T) = \tau_0 \exp(\Delta E_0/k_B T), \quad (7)$$

where ΔE_0 is an effective activation energy. Linear fits for the inset of Fig. 4 yield $\tau_0 \cong 10^{-9}$ s, $\Delta E_0 \cong 0.2$ eV for the faster relaxation, and $\tau_0 \cong 10^{-7}$ s, $\Delta E_0 \cong 0.1$ eV for the slower one. This analysis implies that an electron must overcome a larger energy barrier for the hop that is shorter in distance. This agrees with the suggested role of spin correlations in determining the likelihood of charge hops among nearby sites.

The microwave frequency range conductivity is consistent with the audio frequency ac results (Fig. 2). The microwave frequency dielectric constant data versus T are plotted in Fig. 5. The microwave dielectric constant of an activated dipole oscillator can be estimated as¹⁶

$$\epsilon = \epsilon_\infty + \frac{4\pi n e^2 L^2}{\epsilon_0(1 + \omega^2 \tau^2) k_B T} \exp\left(\frac{-\Delta E_0}{k_B T}\right), \quad (8)$$

where $\epsilon_\infty = 2.6$ is the core dielectric constant, obtained from the data at $T \rightarrow 0$, n is the charge density, and L is the localization length. Taking $\Delta E_0 \sim 1800$ K from a fit to the data in Fig. 5 and $n = 1.5 \times 10^{22}$ cm⁻³ estimated from the x-ray structure study of $V(\text{TCNE})_x \cdot y(\text{CH}_2\text{Cl}_2)$,¹⁷ a localization length L of ~ 5.3 Å is obtained for $\epsilon(300$ K) $\cong 3.18$. This length is comparable with the size of a $[\text{TCNE}]^-$ group, and implies that electrons involved in charge conduction are strongly localized within $[\text{TCNE}]^-$ sites.

CONCLUSIONS

The charge transport studies present self-consistent results in a wide frequency range (0– 10^{10} Hz) on this new

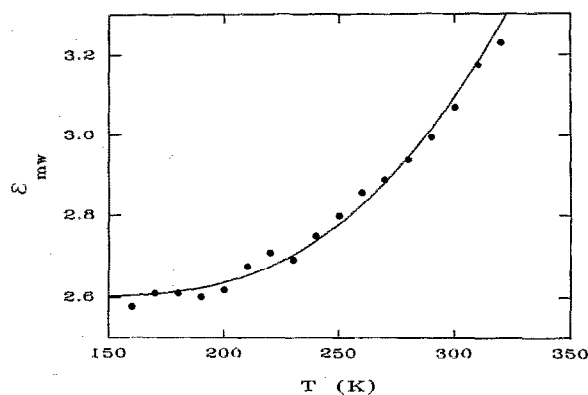


FIG. 5. Temperature dependence of microwave dielectric constant ϵ_{mw} of $V(\text{TCNE})_x \cdot y(\text{CH}_2\text{Cl}_2)$, solid line is a fit to Eq. (8).

high T_c molecular-based magnet $V(\text{TCNE})_x \cdot y(\text{solvent})$. The anomalies detected in the ac transport suggest that the magnetic nature of this material dominates aspects of the charge conduction in this system. In this sense, the charge transport studies are consistent with the magnetic studies of this molecular-based magnet.⁶

ACKNOWLEDGMENTS

The authors thank G. T. Yee and C. Vazquez at Du Pont Company for providing samples, and Dr. P. Zhou at The Ohio State University for useful discussions. This work was supported in part by the DOE under Grant No. DE-FC02-86ER45271.A.

- ¹S. Chittipeddi, K. R. Cromack, J. S. Miller, and A. J. Epstein, *Phys. Rev. Lett.* **58**, 2695 (1987); A. Chakraborty, A. J. Epstein, W. Lawless, and J. S. Miller, *Phys. Rev. B* **40**, 11422 (1989).
- ²J. S. Miller, A. J. Epstein, and W. M. Reiff, *Chem. Rev.* **88**, 201 (1988).
- ³See, for example, O. Kahn, D. Gatteschi, J. S. Miller, and F. Palacio, Eds., *Proceedings of the NATO ARW on Molecular Magnetic Materials*, **E198** (Kluwer, Amsterdam, 1991).
- ⁴J. S. Miller, A. J. Epstein, and W. M. Reiff, *Science* **240**, 40 (1988).
- ⁵J. M. Manriquez, G. T. Yee, R. S. McLean, A. J. Epstein, and J. S. Miller, *Science* **252**, 1415 (1991).
- ⁶P. Zhou, B. G. Morin, A. J. Epstein, and J. S. Miller (unpublished).
- ⁷N. Mott and E. Davis, *Electronic Processes in Non-Crystalline Materials* (Clarendon, Oxford, 1979).
- ⁸I. G. Austin and N. F. Mott, *Adv. Phys.* **18**, 41 (1969).
- ⁹G. Du *et al.* (unpublished).
- ¹⁰R. H. Cole and K. S. Cole, *J. Chem. Phys.* **9**, 341 (1941).
- ¹¹G. Thummes, F. Korner, and J. Kotzler, *Solid State Commun.* **67**, 215 (1988); H. H. S. Javadi, A. Chakraborty, C. Li, N. Theophilou, D. B. Swanson, A. G. MacDiarmid, and A. J. Epstein, *Phys. Rev. B* **43**, 2183 (1991).
- ¹²Z. H. Wang, A. Ray, A. G. MacDiarmid, and A. J. Epstein, *Phys. Rev. B* **43**, 4373 (1991).
- ¹³N. Theophilou, D. B. Swanson, A. G. MacDiarmid, A. Chakraborty, H. H. S. Javadi, R. P. McCall, S. P. Trent, F. Zuo, and A. J. Epstein, *Synth. Met.* **28**, D35 (1989).
- ¹⁴A. J. Epstein, in *Handbook of Conducting Polymers*, edited by T. A. Skotheim (Marcel Dekker, New York, 1986), Vol. 2, p. 1041.
- ¹⁵P. Debye, *Polar Molecules* (Chemical Catalogue Company, New York, 1929).
- ¹⁶H. H. S. Javadi, J. S. Miller, and A. J. Epstein, *Phys. Rev. Lett.* **59**, 1760 (1987).
- ¹⁷Z. Oblakowski, A. J. Epstein, M. Laridjani, J. P. Pouget, and J. S. Miller (unpublished).